Applied Surface Science 401 (2017) 100–105

Contents lists available at ScienceDirect

Applied Surface Science

journal homepage: www.elsevier.com/locate/apsusc

Full Length Article

Synthesis, characterization and frictional wear behavior of ceria hybrid architectures with {111} exposure planes

Pengfei Hu [a], Yong Chen [a,*], Rong Sun [b], Yue Chen [a], Yaru Yin [a], Zhongchang Wang [b,*]

[a] School of Mechanical Engineering, University of South China, Hengyang 421001, China
[b] Advanced Institute for Materials Research, Tohoku University, 2-1-1 Katahira, Aoba-ku, Sendai, Japan

ARTICLE INFO

Article history:
Received 3 November 2016
Received in revised form
16 December 2016
Accepted 2 January 2017
Available online 3 January 2017

Keywords:
CeO_2 microstructure
Hydrothermal process
Hybrid architecture
{111} Exposure Plane

ABSTRACT

A hybrid architecture comprising three types of cerium nanoparticles, nano-octahedron and its ramifications, is synthesized via a facile yet efficient hydrothermal process. Comprehensive transmission electron microscopy analysis identifies the exposure planes of the cube-shaped ceria nanoparticles as {111} crystal planes. As a result of this unique morphology, the nanoparticles are found to show markedly enhanced material removal capacity and inferior polishing quality compared to the sphere-shaped ceria nanoparticles.

1. Introduction

Ceria (CeO_2) particles have received a great deal of attention recently due to their remarkable catalytic activity, polishing performance and ultraviolet absorbents function, and also for their ability to store and transport oxygen [1–6]. Up to now, much effort has been devoted to the controllable synthesis of CeO_2 nanoparticles with a specific size and shape [7–14]. The shape and size of nanocrystals impose significantly impact on their physical and chemical properties [15–18]. In particular, sphere-shaped nanoparticles have attracted extensive interest due to their excellent polishing quality [19–23]. As for CeO_2 spheres, the polishing mechanism is surface grinding because there is no sharp edge. However, the materials removal efficiency of the CeO_2 spheres are rather insufficient. The nanoparticle with a sharp edge may have preferable cutting ability that can enhance the material removal efficiency.

Here, we fabricate a hybrid architecture comprising nano-octahedron and its ramifications cerium nanoparticles with sharp edges via a facile hydrothermal process. The morphologies of CeO_2 nano-octahedron and its ramifications are characterized by field emission scanning electron microscopy (FESEM). We also test the mechanical polishing properties of CeO_2 nanoparticles composed of nano-octahedrons and their ramifications.

2. Experimental

All chemical reagents were of analytical grade (purity: 99.99%) and used without further purification. The CeO_2 nanomaterials were synthesized by the hydrothermal method [24–29]. Cerium nitrate hexahydrate ($Ce(NO_3)_3{\cdot}6H_2O$) and ammonium acetate(CH_3COONH_4) were first dissolved in distilled water, followed by stirring for 15 min with magnetic stirrer to form precursors. The solution was then transferred to autoclaves and treated at 473 K for 24 h under autogenously pressure. Finally, the white products were obtained by centrifuging, washing with distilled water and ethanol to remove unexpected ions, and eventually drying at 333 K in air.

The CeO_2 slurry based on spheres and particles was used for silicon single crystal substrate polishing with a concentration of 2.5 wt%. In the CMP process, the polishing pad was rotated at a very high speed of 2000 rpm. During polishing, a constant load of 10 KPa was applied to the polishing head. The slurry flow rate was 50 ml/min, and the solid content (for abrasive particles) of slurries was 1 wt%. The polishing time was 1 min. Microstructures were characterized using X-ray diffraction (XRD) and scanning electron microscopy (SEM). For XRD, a Rigaku D/max-1200X diffractometry

* Corresponding authors.
E-mail addresses: chenyongjsnt@163.com, 40372167@qq.com (Y. Chen), zcwang@wpi-aimr.tohoku.ac.jp (Z. Wang).

http://dx.doi.org/10.1016/j.apsusc.2017.01.005
0169-4332/

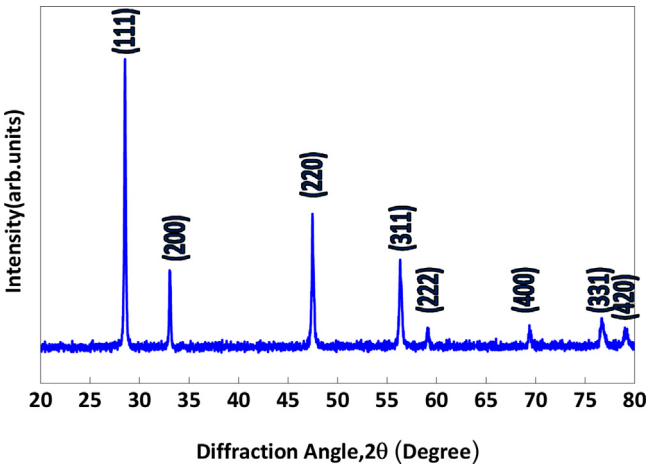

Fig. 1. XRD spectrum of the powder synthesized via the hydrothermal method.

with Cu *Kα* radiation operated at 45 KeV and 200 mA. Morphologies were observed using Hitachi SU-8000SEM and microstructures were further observed by transmission electron microscopy (TEM) (JEM-2010F, JEOL) operated at 200 KeV [30–34].

3. Results and discussion

To determine the phase of the synthesized particles, we conducted XRD analysis. Upon a closer indexing, the diffraction peaks are identified as (111), (200), (220), (311), (222), (400), (331), and (420) lattice planes, which match well with those of the standard CeO_2 with a fluorite structure (Fig. 1). From Fig. 2(a), one can confirm the hybrid systems of particles with two utterly different sizes prepared with the facile hydrothermal technique. The small particles have an average size of less than 30 nm, while the larger ones have a size of up to ~100 nm, exhibiting a morphology with well-defined edges. Fig. 2(b) and (c) shows morphology of the octahedron and its ramification. Surfaces of the nano-particles are clean and smooth. To gain insights into structure of the nanoparticles, we carry out TEM analyses. Fig. 3(a) (d) and (g) shows a bright-field TEM image of three typical pristine CeO_2 nano-octahedron and its ramifications and the inset shows corresponding morphology of CeO_2 nanoparticles. Further selected-area diffraction patterns (SADP) identify the nano-octahedron and its ramification as face-centered cubic CeO_2 (Fig. 3(b)(e)(h)). Fig. 3 (b) (e) and (h) presents the SADP of the CeO_2 nano-octahedron and its ramification, from which the diffraction spots of FCC-CeO_2 are identified along $[1\bar{1}0]$ (Fig. 3(e) and (h)) and (211) zone axis (Fig. 3(b)). Fig. 3(c), (f), (i) shows typical high-resolution TEM (HRTEM) images taken at a corner of each samples, from which lattice spacing is determined to be ~0.31 nm, in line with that of the (111) planes of CeO_2, thereby confirming that the nano-octahedrons is terminated with {111} planes [35,36]. The exposure planes of octahedron are shown in Fig. 4. All exposure planes of octahedron are {111} planes in terms of structural crystallography (Fig. 4(a)). The octahedron's ramification is stretched along [001] direction. The surfaces of nano-octahedrons and its ramification are thus confirmed to be composed of {111} crystal planes (Fig. 4(b)).

We calculate the distance between different crystal planes (*hkl*), h_{hkl} by the Bravais theory [37] to elucidate growth origin of the nano-octahedrons [12]. Our calculations show that the growth rate of plane R_{111} is lowest and the {111} planes of CeO_2 are prone to be exposed. This means that CeO_2 octahedrons and ramifications are formed in an easy fashion.

Based on the aforementioned observations and calculations, we propose a possible growth mechanism for the two types of ceria products (nano-octahedron and its ramification). First, the mineralizer CH_3COONH_4 produces OH^- ions by ionization reaction, as given in Reaction (1) and (2). Then, the OH^- ions react with Ce^{3+} ions to form milky $Ce(OH)_3 \cdot nH_2O$ precipitates (Reactions (3)), In hydrothermal process, the $Ce(OH)_3 \cdot nH_2O$ precursors are oxidized at high temperature and pressure, generating nucleation of CeO_2 particles, as shown in Reaction (4). The nucleated CeO_2 crystals are grown along a particular direction, forming well-defined nano-octahedrons with {111} exposure planes. Some octahedral-shaped CeO_2 crystals keep growing to form octahedron of a large size. A part of CeO_2 nano-octahedrons continue growing along their body diagonal ([001]) direction, evolving to octahedron's ramifications.

$$CH_3COO^- + NH_4^+ + H_2O \leftrightarrow CH_3COOH + NH_3 \cdot H_2O \quad (1)$$

$$NH_3 \cdot H_2O \leftrightarrow NH_4^+ + OH^- \quad (2)$$

$$Ce^{3+} + 3OH^- + nH_2O \rightarrow Ce(OH)_3 \cdot nH_2O \quad (3)$$

$$4Ce(OH)_3 \cdot nH_2O + O_2 \rightarrow 4CeO_2 \cdot nH_2O + 4H_3O^+ + 2O^{2-}. \quad (4)$$

It is well-known that ceria acts as one of the most important materials for polishing. To investigate how the exposure planes impact the polishing properties of CeO_2 nanoparticles, we measure polishing properties of the sphere-shaped (exposed with nonspecific crystal planes) CeO_2 nanoparticles together with octahedron-shaped (exposed with {111} crystal planes) nanoparticles. The synthesis process and structural characterization for the sphere-shaped nanoparticles have been reported in our previous work [14]. Fig. 5 shows SEM images of the silicon single crystal substrate polished by the sphere- and octahedron-shaped CeO_2 nanoparticles. From Fig. 5(a), the shadow scratches and holes are found on surfaces of the silicon single crystal substrate due to the sphere-shaped CeO_2 nanoparticles. The deep ploughing traces (marked with arrows) could be detected on the surface of silicon single crystal substrate polished by the octahedron-shaped CeO_2 nanoparticles under a low sliding speed and light-load as shown in Fig. 5(b). To shed light on how the interface between the silicon single crystal substrate and CeO_2 nanoparticles affect the polish quality and removal efficiency, compressive stress distribution calculations are conducted using the finite element analysis (FEA). The three-dimensional FEA result shows that the maximum compressive stress of the silicon single crystal substrate is 61893 MPa due to the point contact between the CeO_2 nano-spheres and silicon substrate (Fig. 6(a)). The maximum compressive stress of silicon substrate in case of nano-particles shaped with octahedron and its ramification is 24198 and 31194 MPa, respectively (Fig. 6(d), (b))